Available online at www.sciencedirect.com
SCIENCE DIRECT®
Journal of Sound and Vibration 268 (2003) 115–129
JOURNAL OF SOUND AND VIBRATION
www.elsevier.com/locate/jsvi

Dynamics modelling of beams with shunted piezoelectric elements

C.H. Park*

Department of Mechanical Engineering, Pohang University of Science and Technology, POSTECH, San 31 Hyoja-dong Namgu, Pohang 790-784, South Korea

Received 27 February 2002; accepted 8 November 2002

Abstract

General modelling of a resonant shunting damper has been made from piezoelectric sensor/actuator equations. It is found that an additional damping, which is augmented to a system, is generated by the shunt damping effect. The transfer function of the tuned electrical absorber is derived for both series and parallel shunt circuit. The governing equations and associated boundary conditions are derived using Hamilton's principle. The shunt voltage equation is also derived from the charge generated in PZT due to beam vibration. The frequency response function of the obtained mathematical model is compared with that of the tuned electrical absorber and experimental work. The vibration amplitude is reduced about 15 dB at targeted second mode frequency.

1. Introduction

Structural vibration suppression via piezoelectric shunt circuits has been of popular interest in recent years due to light weight, ease of use, and good performance. Also, compared with mechanical passive damping (viscoelastic material damping), piezoelectric shunted network is less temperature dependent [1]. There are many kinds of shunt circuits such as resistive, inductive, capacitive, and switched [2]. Each type of shunts has different characteristics to be exploited. We focus on the inductive shunt circuit for vibration suppressions. An inductive shunt circuit results in a resonant inductor–capacitor (LC) circuit; thus, it is called the resonant shunt circuit, whose behavior is analogous to that of a mechanical vibration absorber. The resonant shunt circuit consists of three components: a capacitor, a resistor and an inductor. The resistor–inductor (R–L)

*Corresponding author. Tel.: +82-54-279-2962; fax: +82-54-297-5899.
E-mail address: drparkch@postech.ac.kr (C.H. Park).

0022-460X/03/$ - see front matter
doi:10.1016/S0022-460X(02)01491-8

circuit, connected in series or in parallel, has dynamics similar to that of a mechanical vibration absorber. Following the principle of a mechanical absorber, the resonant shunt must be tuned correctly to absorb the vibration energy of the system's target mode.

As shown in Fig. 1, the two external terminals of the PZT, modelled as a capacitor (the piezoelectric element behaves electrically as a capacitor and a voltage source), are connected to (a) the series or (b) parallel inductor and resistor branch shunt circuit. The piezoceramic element is used to convert mechanical energy of a vibrating structure into electrical energy by direct piezoelectric effect. This electric energy is dissipated as Joule heating through the shunting resistor efficiently when the electrical resonant frequency matches the mechanical frequency. At resonance, the reactive components between the LC cancel each other and the phase between the current and voltage is zero. As a result, the power factor at resonance becomes one.

Many researchers have developed theoretical analyses to represent the mechanism of shunting damper. Hagood and von Flotow [3] presented the general shunted model for two shunt circuits: the case of resistor alone and that of a RL connected in series. For resistive shunting, the material properties exhibit frequency dependence similar to viscoelestic material. Law et al. [4] developed a new model as considering the energy conversion and dissipation to characterize the damping behavior of the piezo materials. Equations were derived to predict optimal resistance load, maximum damping ratio and the shift of the resonance frequency. Tsai and Wang [5] presented the active–passive hybrid piezoelectric network. The shunt circuit not only can provide passive damping, it can also enhance the active action authority if tuned correctly. Saravanos [6] developed mechanics for the analysis of damping in composite plates with multiple resistively shunted piezoelectric layers. He showed that substantial vibration control of selected modes could

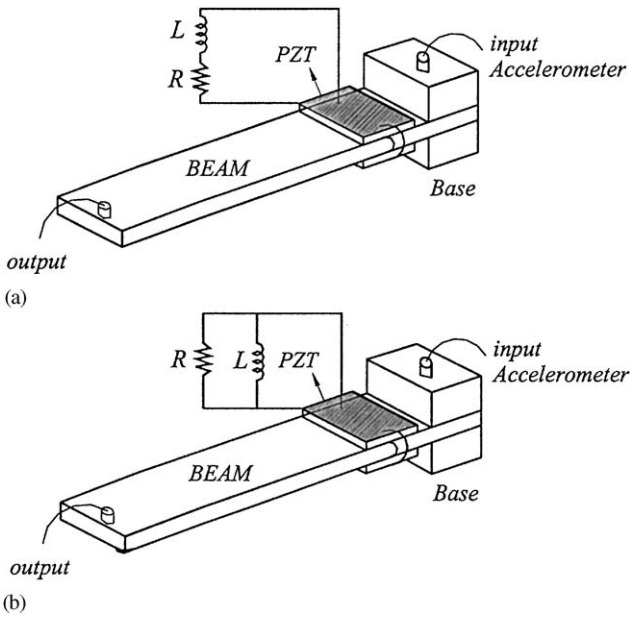

Fig. 1. Schematic drawings of experimental setup for: (a) a series R–L and (b) a parallel R–L shunt circuit.

be obtained by proper tuning of the resistive shunt circuit. Kim et al. [7] developed a finite element code to represent active and passive schemes for non-linear flutter of composite panel. The effects of vibration suppression by using a series R–L shunt circuit were investigated.

In this paper, the general modelling of the resonant shunting damper is presented, in which shows the additional damping mechanism generated by the shunt damping effect. The transfer function of the tuned electrical absorber is derived for both series and parallel R–L shunt branch circuit. A cantilever beam with a pair of PZT patches is used to demonstrate theoretically and experimentally the resonant shunt damping capabilities. The equations of motion and associated boundary conditions of the shunted piezo/beam system are formulated using Hamilton's principle. Assumed series shape functions, which satisfy the boundary conditions, are used to analyze the flexural motion of the cantilevered beam. The theoretical model obtained is validated experimentally. The obtained results suggest that resonant shunting damper provides an effective means for vibration control.

2. General modelling of resonant shunt circuit

The piezo shunt circuit generates an additional damping matrix which can be augmented to the equation of motion of a structure system. A pair of piezoelectric actuator/sensor equations [8] is used to derive an additional shunt damping matrix:

Actuator equations:

$$M\ddot{w} + C\dot{w} + Kw = f_{ext} + \theta V_{SH}, \tag{1}$$

Sensor equations:

$$q = \theta^{\mathrm{T}} w + C_p V_{SH}, \tag{2}$$

where M, C, and K are the mass, damping, and stiffness matrices of the piezo/beam system measured at constant electrical field (e.g., short circuit). Hence, the system stiffness consists of a base structure stiffness and a short-circuited piezoelectric stiffness, that is, $K = K_s + K_p^E$. In the sensor equation, q is the piezoelectric charge matrix and θ is the electromechanical coupling matrix. This piezoelectric actuator/sensor equation accounts for the effects of dynamic coupling between a structure and an electrical network through the piezoelectric effect. A current equation can be obtained as differentiating the sensor Eq. (2). Substituting it into the shunt voltage equation as shown in Fig. 2, we can define the shunt voltage equation as follows [9]:

$$\begin{aligned} V_{SH} &= -Z_{SH} I \\ &= -Z_{SH}(\theta^{\mathrm{T}}\dot{w} + C_p^{\mathrm{T}}\dot{V}_{SH}) \\ &= -Z_{SH}\theta^{\mathrm{T}} sw - Z_{SH} C_p s V_{SH}, \end{aligned} \tag{3}$$

where s is the Laplace parameter. Therefore, the new defined shunt voltage can be

$$V_{SH} = \frac{-Z_{SH}\theta^{\mathrm{T}} sw}{1 + Z_{SH} C_p s}. \tag{4}$$

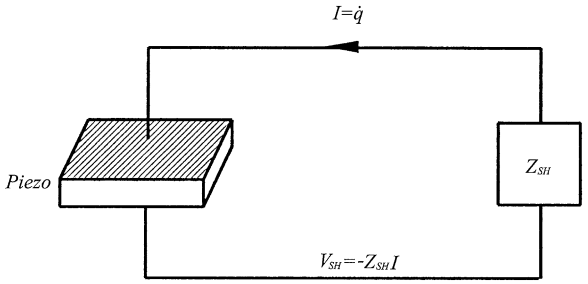

Fig. 2. Feedback current into a PZT due to shunt impedance.

Substituting Eq. (4) into the actuator Eq. (1), the governing equation of a shunted system can be augmented by adding the shunt damping matrix in the Laplace domain:

$$Ms^2w + \left(C + \frac{Z_{SH}\theta\theta^{\mathrm{T}}}{1 + Z_{SH}C_p s}\right)sw + Kw = f_{ext}(s). \tag{5}$$

By dividing the both sides in Eq. (5) by the system stiffness, K, we can rewrite Eq. (5) as follows:

$$\left(\frac{M}{K}s^2 + \frac{C}{K}s + 1 + \frac{\theta\theta^{\mathrm{T}}}{C_p K}\frac{Z_{SH}C_p s}{1 + Z_{SH}C_p s}\right)w(s) = \frac{f_{ext}(s)}{K}. \tag{6}$$

To obtain a position transfer function of a shunted system, the following parameters are used:

$$\omega_n^E = \sqrt{\frac{K}{M}}, \quad \gamma = \frac{s}{\omega_n^E}, \quad \frac{C}{K}s = 2\xi\gamma, \quad \hat{Z} = Z_{SH}C_p s, \quad K_{ij}^2 = \frac{\theta\theta^{\mathrm{T}}}{C_p K}, \tag{7}$$

where ω_n^E is a natural frequency of a mechanical system with the short-circuited piezoelectric material, γ is a non-dimensional frequency, and K_{ij} is a generalized electromechanical coupling constant. By using the parameters defined above, Eq. (6) can be rewritten as

$$\left(\gamma^2 + 2\xi\gamma + 1 + K_{ij}^2\frac{\hat{Z}}{1 + \hat{Z}}\right)w = w_{st}. \tag{8}$$

The transfer function of a mechanical structure with the shunted piezoelectric material is

$$\frac{w}{w_{st}} = \frac{1 + \hat{Z}}{(1 + \hat{Z})(\gamma^2 + 2\xi\gamma + 1) + K_{31}^2\hat{Z}}. \tag{9}$$

2.1. Series inductor and resistor shunt branch circuit

The impedance of a series R–L branch circuit is obtained from Fig. 3(a)

$$Z_{SH}^{se} = Ls + R. \tag{10}$$

The generalized resonant impedance for a series R–L shunt, $\hat{Z}$, is given by

$$\hat{Z} = Z_{SH}^{se}C_p s = \frac{s}{\omega_n^E}Z_{SH}^{se}C_p\omega_n^E = \gamma^2 LC_p(\omega_n^E)^2 + RC_p\omega_n^E\gamma = \frac{1}{\delta^2}(\gamma^2 + r\gamma\delta^2), \tag{11}$$

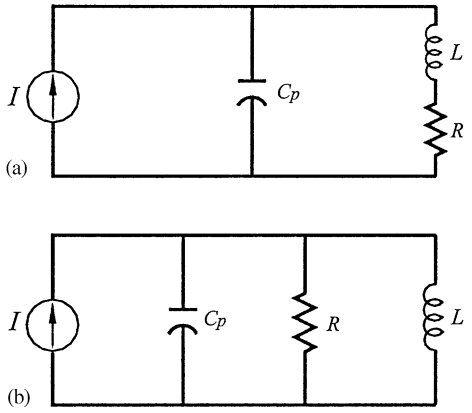

Fig. 3. Circuit models of piezoceramic with a series R–L and a parallel R–L shunt circuit.

where $\delta = 1/\sqrt{LC_p\omega_n^E}$ and $r = RC_p\omega_n^E$. The δ parameter is the non-dimensional turning ratio for which the electrical resonant frequency is tuned in the vicinity of a mechanical resonant frequency. Substituting $\hat{Z}$ into Eq. (9) results in the final form of a system transfer function with an inherent structural damping as follows:

$$\frac{w}{w_{st}} = \frac{\delta^2 + r\gamma\delta^2 + \gamma^2}{(\delta^2 + r\gamma\delta^2 + \gamma^2)(\gamma^2 + 2\xi\gamma + 1) + K_{31}^2(\gamma^2 + r\gamma\delta^2)}. \tag{12}$$

2.2. Parallel inductor and resistor shunt branch circuit

Following the above procedure, the transfer function with a parallel R–L shunt branch circuit can be described. The impedance of a parallel R–L branch circuit can be expressed in Laplace form by

$$Z_{SH}^{pa} = \frac{LRs}{Ls + R}. \tag{13}$$

The generalized resonant impedance for a parallel R–L shunt is given by

$$\hat{Z} = Z_{SH}^{pa}C_p s = \frac{s}{\omega_n^E}Z_{SH}^{pa}C_p\omega_n^E = \frac{\gamma rLs}{Ls + R} = \frac{\gamma^2 rL\omega_n^E}{L\omega_n^E\gamma + R} = \frac{\gamma^2 r}{\gamma + r\delta^2}. \tag{14}$$

Substituting Eq. (14) into Eq. (9) generates the transfer function for a parallel R–L shunted piezoceramic and structure

$$\frac{x}{x^{ST}} = \frac{\gamma^2 r + \gamma + r\delta^2}{(\gamma^2 r + \gamma + r\delta^2)(\gamma^2 + 2\xi\gamma + 1) + K_{31}^2(\gamma^2 r)}. \tag{15}$$

3. Equations of motion of the piezo/beam system

A mathematical model is developed to describe the flexural vibration behavior of a cantilevered beam system with resonant shunt circuits. The equations of motion of an piezo/beam system are obtained through Hamilton's principle. A schematic configuration of a piezo/beam system with a series and a parallel shunt circuit is shown in Fig. 1. The beam has length l_b, width b_b, thickness h_b, Young's modulus E_b, and mass density ρ_b. The PZT-5H has thickness h_p, elastic modulus measured at constant electrical field E_p^E, and piezoelectric constants d_{31} in the longitudinal direction.

It is assumed that the transverse displacement, w, of all points on any cross-section of piezo/beam layers is considered to be equal. Shear deformation and rotary inertia of the beam and piezo layers are not included. For symmetry configuration of PZT patches, the net longitudinal displacement of beam is assumed zero. In addition, the base beam layer and the piezoceramic layers are considered to be perfectly bonded together.

The constitutive equation for a piezoelectric element [10] depends on the mechanical stress, σ, and strain, ε, as well as the electric field, E, and the electric displacement, D. A common form of constitutive equations, especially, for a passive shunt damping is

$$\begin{bmatrix} \sigma \\ E \end{bmatrix} = \begin{bmatrix} E_s & -h \\ -h & \beta \end{bmatrix} \begin{bmatrix} \varepsilon \\ D \end{bmatrix}, \tag{16}$$

where E_s is the elastic modulus at the constant displacement, h is the piezoelectric constant, and β is the dielectric constant.

The kinetic energy of a piezo/beam system can be described as

$$T = T_b + 2T_p, \tag{17}$$

where

$$T_b = \frac{1}{2}\int_0^{l_b} \rho_b A_b \left(\frac{\partial w}{\partial t}\right)^2 \mathrm{d}x$$

and

$$T_p = \frac{1}{2}\int_0^{l_b} \rho_p A_p \left(\frac{\partial w}{\partial t}\right)^2 [\mathrm{H}(x - x_1) - \mathrm{H}(x - x_2)]\,\mathrm{d}x.$$

The strain energy of a piezo/beam system can be described as

$$U = U_b + 2U_p, \tag{18}$$

where

$$U_b = \frac{1}{2}\int_0^{l_b} E_b I_b \left(\frac{\partial^2 w}{\partial x^2}\right)^2 \mathrm{d}x$$

and

$$U_p = \frac{1}{2}\int_V (\varepsilon^{\mathrm{T}}\sigma + ED)\,\mathrm{d}V$$
$$= \frac{1}{2}\int_0^{l_b}\left[E_p^E I_p\left(\frac{\partial^2 w}{\partial x^2}\right)^2 + 2bh_{31}Dz_n\left(\frac{\partial^2 w}{\partial x^2}\right) + A_p\beta_{33}D^2\right][\mathrm{H}(x-x_1) - \mathrm{H}(x-x_2)]\,\mathrm{d}x,$$

where $z_n = \frac{1}{2}h_p(h_b + h_p)$ and H is the Heaviside's function. Also, A_b and A_p are the cross-sectional area of beam and piezo layer, respectively. Furthermore, I_b and I_p are the area moment of inertia about the neutral axis of each layer. In the above equations, $(x_2 - x_1)$ is the length of the PZT patch. The subscripts b and p represent the base beam and piezoceramic, respectively. The virtual work consists of three terms: the first term is for work done by the piezo resonant damper, the second is due to the external force, and the third is due to the inherent damping force of a base structure.

In series case,

$$\delta W = (Ls + R)\dot{Q}\delta Q\Delta\mathrm{H} + \int_0^{l_b} f(x,t)\delta w\,\mathrm{d}x - \int_0^{l_b} c_b\frac{\partial w}{\partial t}\delta w\,\mathrm{d}x. \tag{19}$$

In parallel case,

$$\delta W = \left(\frac{LRs}{Ls+R}\right)\dot{Q}\delta Q\Delta\mathrm{H} + \int_0^{l_b} f(x,t)\delta w\,\mathrm{d}x - \int_0^{l_b} c_b\frac{\partial w}{\partial t}\delta w\,\mathrm{d}x, \tag{20}$$

where $\Delta\mathrm{H} = [\mathrm{H}(x-x_1) - \mathrm{H}(x-x_2)]$ and Q is the electric charge generated by an external force.

The equations of motion and all the natural and geometric boundary conditions can be obtained by applying Hamilton's principle

$$\delta\mathrm{H} = \delta\int_{t_1}^{t_2}(T - U + W)\,\mathrm{d}t = 0, \tag{21}$$

where t_1 and t_2 are the end points in the time domain and δ is the virtual work parameter. Substituting the strain energy and kinetic energy into Hamilton's principle yields the following equations of motion and electrical circuit equation:

$$\rho_b A_b\left(\frac{\partial^2 w}{\partial t^2}\right) + c_b\left(\frac{\partial w}{\partial t}\right) + E_b I_b\left(\frac{\partial^4 w}{\partial x^4}\right) + 2\left[\rho_p A_p\left(\frac{\partial^2 w}{\partial t^2}\right) + E_p^E I_p\left(\frac{\partial^4 w}{\partial x^4}\right)\right][\mathrm{H}(x-x_1) - \mathrm{H}(x-x_2)]$$
$$= f(x,t) - b_p h_{31} D_3 h_p(h_b + h_p)\left(\frac{\partial^2}{\partial x^2}[\mathrm{H}(x-x_1) - \mathrm{H}(x-x_2)]\right). \tag{22}$$

The electrical circuit equations in series and in parallel shunt circuit are

$$\left[h_{31}h_p(h_b+h_p)\left(\frac{\partial^2 w}{\partial x^2}\right) + \frac{2\beta_{33}h_p}{bl_p}Q - (Ls+R)\dot{Q}\right][\mathrm{H}(x-x_1) - \mathrm{H}(x-x_2)] = 0, \tag{23}$$

$$\left[h_{31}h_p(h_b+h_p)\left(\frac{\partial^2 w}{\partial x^2}\right) + \frac{2\beta_{33}h_p}{bl_p}Q - \left(\frac{LRs}{Ls+R}\right)\dot{Q}\right][\mathrm{H}(x-x_1) - \mathrm{H}(x-x_2)] = 0. \tag{24}$$

The first terms of Eqs. (23) and (24) define the sensor voltage generated by the curvature of the deformed beam. The second terms are due to an inherent capacitance of a pair of PZT. The third terms are defined as shunt voltages.

The assumed mode method is used to discretize the governing Eq. (22) into a set of ordinary differential equation. The flexural motion for a cantilever beam is approximated by

$$w(x,t)=\sum_{i=1}^{n}\psi_i(x)W_i(t)=[\psi]^{\mathrm{T}}[\mathrm{W}], \tag{25}$$

where $\psi_i(x)=\cos\beta_i x-\cos\beta_i x-\sigma_i(\sinh\beta_i x-\sin\beta_i x)$. Here the constants σ_i are the mode shape coefficients [11]. Applying mode shape functions to the equation of motion (22) results in the following discretized differential equations of the piezo/beam system:

$$M\ddot{W}(t)+C_b\dot{W}(t)+KW(t)=f_{ext}+f_{piezo}, \tag{26}$$

where

$$M=\rho_b A_b\int_0^l \psi_i\psi_i^{\mathrm{T}}\,\mathrm{d}x+2\rho_p A_p\int_0^l \psi_i\psi_i^{\mathrm{T}}[\mathrm{H}(x-x_1)-\mathrm{H}(x-x_2)]\,\mathrm{d}x,$$

$$C_b=c_b\int_0^l \psi_i'\psi_i'\mathrm{T}\,\mathrm{d}x,$$

$$K=E_bI_b\int_0^l \psi_i''\psi_i''^{\mathrm{T}}\,\mathrm{d}x+2E_p^E I_p\int_0^l \psi_i''\psi_i''^{\mathrm{T}}[\mathrm{H}(x-x_1)-\mathrm{H}(x-x_2)]\,\mathrm{d}x,$$

$$f_{ext}=\int_0^l \psi_i f(x,t)\,\mathrm{d}x,$$

$$f_{piezo}=-b_p d_{31}E_p^E V_{SH}(h_b+h_p)\int_0^l \psi_i\left[\delta'(x-x_1)-\delta'(x-x_1)\right]\mathrm{d}x,$$

where d_{31} is the piezoelectric material constant. Moreover, Hamilton's principle yields the following boundary conditions:

Geometric boundary conditions:

$$w=0,\quad \frac{\partial w}{\partial x}=0. \tag{27}$$

Natural boundary conditions:

$$\begin{aligned}
&E_bI_b\left(\frac{\partial^2 w}{\partial x^2}\right)+2E_pI_p\left(\frac{\partial^2 w}{\partial x^2}\right)[\mathrm{H}(x-x_1)-\mathrm{H}(x-x_2)]\\
&\quad=-b_ph_{31}D_3h_p(h_b+h_p)[\mathrm{H}(x-x_1)-\mathrm{H}(x-x_2)],\\
&E_bI_b\left(\frac{\partial^3 w}{\partial x^3}\right)+2E_pI_p\left(\frac{\partial^3 w}{\partial x^3}\right)[\mathrm{H}(x-x_1)-\mathrm{H}(x-x_2)]\\
&\quad=-b_ph_{31}D_3h_p(h_b+h_p)[\delta(x-x_1)-\delta(x-x_2)].
\end{aligned} \tag{28}$$

These boundary conditions render the solution of the differential equation of piezo/beam system unique. Eq. (28) shows how the bending moment and the shear force generated by the electromechanical interactions of the piezoelectric material affects the natural boundary condition of the piezo/beam system.

The charge generated by the PZT patches due to the vibration of the cantilever beam can be determined from the electric field displacement, $\{D\}$:

$$Q(t) = \int_A D \, \mathrm{d}A, \tag{29}$$

with

$$\{D\} = [d]^{\mathrm{T}}\{T\} + [\varepsilon]^{\mathrm{T}}\{E\}, \tag{30}$$

where $[d]$, $\{T\}$, $[\varepsilon]$ and $\{E\}$ represent the piezoelectric strain constant, stress, dielectric permittivity and applied field strength matrix, respectively [10]. Substituting the mode shape function into Eq. (29), the output of a piezo sensor can be derived as follows:

$$Q_i(t) = (C_0 D_n + C_p^{\mathrm{T}} V_{SH})[\mathrm{H}(x - x_1) - \mathrm{H}(x - x_2)], \tag{31}$$

where

$$C_0 = d_{31} E_p^E b_p \left(\frac{h_b}{2} + h_p\right) \quad \text{and} \quad D_n = \int_0^l \frac{\partial^2 \psi_i}{\partial^2 x}[\mathrm{H}(x - x_1) - \mathrm{H}(x - x_2)] \, \mathrm{d}x.$$

The current across PZT electrodes can be obtained from the induced charge of the piezoceramic sensor as follows:

$$I_i(t) = \frac{\mathrm{d}Q_i}{\mathrm{d}t} = \left(C_0 D_n \dot{W}_n(t) + C_p^{\mathrm{T}} \dot{V}_{SH}\right)[\mathrm{H}(x - x_1) - \mathrm{H}(x - x_2)]. \tag{32}$$

According to Eq. (3), the shunt voltage is given by:

In series shunt case,

$$V_{SH}^{se} = -Z_{SH}^{se} I_i(t) = -(Ls + R)\left\{C_0 D_n \dot{W}_n(t) + C_p^{\mathrm{T}} s V_{SH}\right\}[\mathrm{H}(x - x_1) - \mathrm{H}(x - x_2)]. \tag{33}$$

In parallel shunt case,

$$V_{SH}^{pa} = -Z_{SH}^{pa} I_i(t) = -\frac{LRs}{(Ls + R)}\left\{ C_0 D_n \dot{W}_n(t) + C_p^{\mathrm{T}} s V_{SH}\right\}[\mathrm{H}(x - x_1) - \mathrm{H}(x - x_2)]. \tag{34}$$

The shunt voltage can be rewritten in series R–L and in parallel R–L case

$$V_{SH}^{se} = -\frac{Ls + R}{LC_p s^2 + RC_p s + 1} C_0 D_n \dot{W}_i(t), \tag{35}$$

$$V_{SH}^{pa} = -\frac{LRs}{LRC_p s^2 + Ls + R} C_0 D_n \dot{W}_i(t). \tag{36}$$

Substituting these shunt voltages into the piezo force, f_{piezo}, in Eq. (26), the final forms of governing equations are given by

$$M\ddot{W}(t) + C_{total}\dot{W}(t) + KW(t) = f_{ext}, \tag{37}$$

where $C_{total} = C_b + f_{piezo}$. It should be noticed that Eq. (37) corresponds to Eq. (5).

4. Experimental implementation

Experiments are performed to examine the behavior of the two different resonant shunt circuits. A pair of piezoceramics, PZT 5H (2.54 cm × 4.5 cm) bonded to each side of the root of the aluminum beam (which is 20 cm long and 2.54 cm wide) by using epoxy adhesives. This edge of the piezoceramic was 0.1 cm away from a fixed end of the beam. This end was clamped vertically to an electro-magnetic shaker. An accelerometer was centered at the free end of the beam to measure system output response. The pair of piezoceramics was poled through their thickness and elongate lengthwise so that they are operating in transverse mode (d_{31}). The beam is grounded and wired in parallel to produce opposite fields in the top and bottom piezoceramics. This causes a moment on the beam when the top PZT contracts as the bottom one expands. Tables 1 and 2 show the physical and geometrical parameters of the aluminum beam and PZT 5H.

The internal function generator of the spectrum analyzer is used to generate a random base acceleration from 1 to 200 Hz with a spectral resolution 0.125 Hz. This random signal is used to excite the beam, which is mounted on an electro-magnetic shaker being driven through a power amplifier. The input signal is measured by an accelerometer, which is attached to an APS shaker. The tip dynamic response (output signal) of the beam is measured by an accelerometer and is fed to the spectrum analyzer to determine its frequency content. Thus, the transfer function between the input and output is obtained.

An active filter [12] is used as a synthetic inductor in the shunt circuit as shown in Fig. 4. The advantages of this inductor are due to its convenience, light weight, and its ability to generate various inductances. R_4 is ordinarily a capacitor, with the other impedances being replaced by resistors, creating an inductor $L = R^*C$, where $R^* = R_1R_3R_5/R_2$. By changing the variable resistor R_2, various inductor values can be obtained.

Several experimental parameters must be determined before conducting an experiment. The open circuit capacitor value (constant stress) of the PZT-5H of 2.0E−7 nF is measured by using an impedance analyzer. The generalized electromechanical coupling constant for a piezoelectric bonded to a structure can be obtained from the frequency change of the electric boundary

Table 1
Physical and geometrical properties of the beam and PZT-5H

Material	Young's modulus (Pa)	Density (kg/m^3)	Poisson ratio (v)	Thickness (m)
Aluminum	7.1E10	2700	0.33	0.8E−3
PZT-5H	6.2E10	7800	0.3	2.6E−4

Table 2
Main piezoelectric parameters of the PZT-5H

d_{31} (m/V)	Polarization field (V/M)	Coupling coefficient, k_{31}	K_3^T, dielectric constant	g_{31} (Vm/N)	Curie temperature (°C)
−320E−12	1.5E6	0.44	3800	−9.5E−3	250

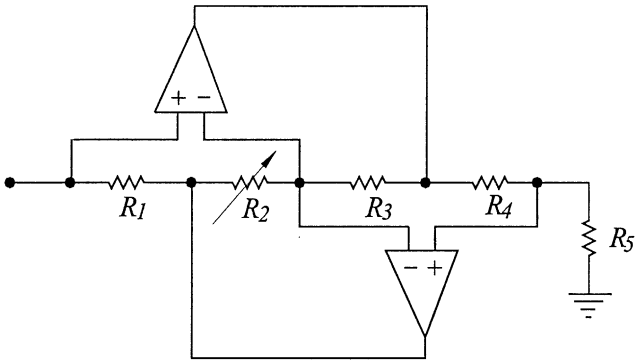

Fig. 4. Circuit diagram of a synthetic inductor.

conditions [3]

$$K_{31}^2 = \frac{(\omega_n^D)^2 - (\omega_n^E)^2}{(\omega_n^E)^2}, \tag{38}$$

where ω_n^D and ω_n^E are the natural frequencies of the structural mode of interest with an open- and a short-circuit piezoceramic, respectively. These frequencies can be obtained from the frequency response function. Here, ω_n^D and ω_n^E are 102.5 and 101.5 Hz, respectively. The generalized electromechanical coupling constant in transverse mode is 0.14.

5. Results and discussions

The series and the parallel resonant shunting damper are both applied experimentally to reduce the second mode vibration amplitude of the cantilever beam. Fig. 5(a) shows experimental results for the series R–L shunt circuit. The vibration amplitude decreases as the shunting resistance decreases. The used resistor values for the series R–L shunt are tabulated in the left column of Table 3. On the contrary, increasing resistance results in improving the vibration attenuation of the parallel R–L shunt as shown in Fig. 5(b). The resistor values are in the right column of Table 3. This phenomenon is easily explained by considering the characteristics of series and parallel R–L–C circuit. If the shunting resistor reaches infinity in the series R–L shunt circuit, the current does not flow. This is referred to as an open circuit. However, it is evident that the parallel shunt circuit would be open (energy does not dissipate), as the shunting resistor value reaches near zero. When the peak becomes a flat plateau, we refer to this as an optimum. As the electronic damping increases further, the two peaks rise up in both cases, exactly as in the case of a mechanical absorber. From Fig. 5, the passive electronic shunt damping is found to produce 15 dB reduction from the peak vibration amplitude of the open circuit. Figs. 6(a) and (b) show the transfer functions of the general model for the series (Eq. (12)) and parallel (Eq. (15)) shunt circuit. The frequency response function of the governing Eq. (37) of the piezo/beam system is also shown in Fig. 7. The shunting resistances predicted by the theoretical models are in good agreement with those obtained by experiment. Table 3 shows a comparison between the theoretical and

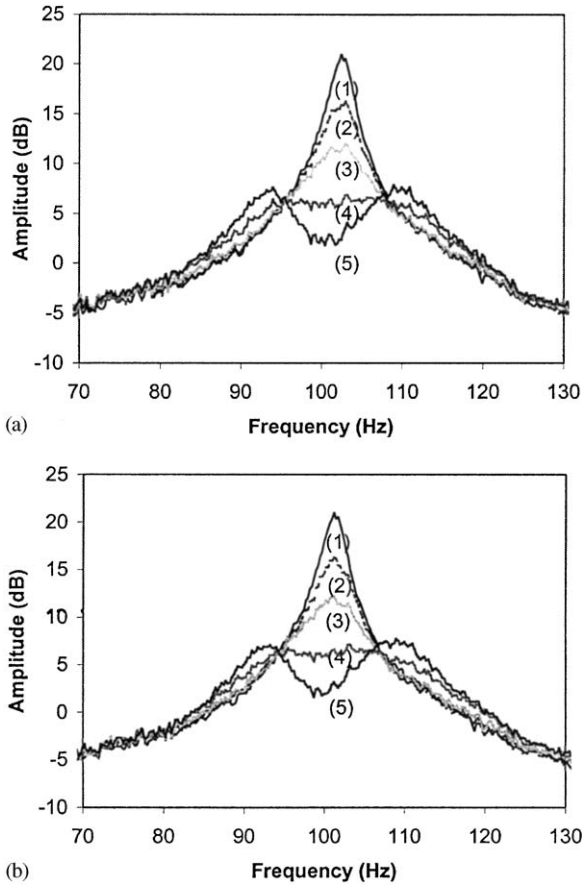

Fig. 5. Experimental transfer response of the piezo/beam system: (a) a series R–L and (b) a parallel R–L shunt circuit.

Table 3
Comparison between theoretical and experimental shunting resistor values

Series R–L shunt circuit			Parallel R–L shunt circuit		
Experiment (Ω)	Tuned electrical model, Eq. (12) (Ω)	Theoretical model (Ω)	Experiment (Ω)	Tuned electrical model, Eq. (15) (Ω)	Theoretical model (Ω)
Open (1)[a]	500,000	500,000	Open (1)[a]	1000	1000
9190 (2)	9190	9500	8030 (2)	8030	8030
3553 (3)	3553	4000	18,430 (3)	18,430	18,430
1359 (4)	2500	2500	48,100 (4)	40,100	35,000
687 (5)	1500	1500	98,300 (5)	75,300	70,500

[a](1), (2), (3), (4), and (5) are the numbers in Figs. 5–7.

experimental resistor shunting values. The error percentage is averagely less than 7.8% between experiment and the tuned electrical absorber model and 15% between experiment and theoretical analysis by using the assumed series method.

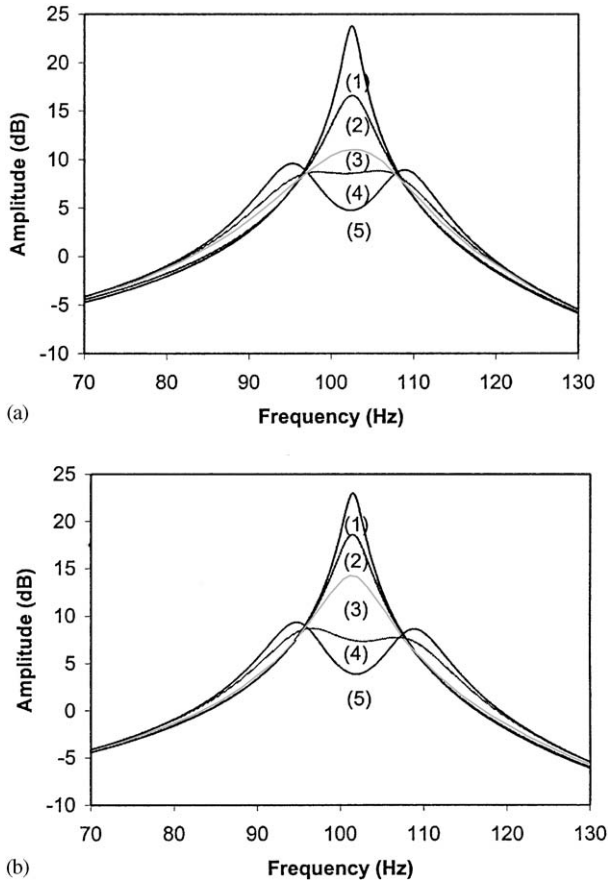

Fig. 6. Transfer response of the tuned electrical absorber by using Eqs. (12) and (15): (a) a series R–L and (b) a parallel R–L shunt circuit.

6. Conclusions

The general modelling of the tuned electrical absorber is developed to describe an additional damping which can be augmented to the equation of motion of the piezo/beam system. A mathematical model is also developed to describe the flexural vibrations of the cantilevered piezo/beam system by using assumed series displacement shape functions. The shunt voltage was formulated from the charge generated by the piezoceramic due to beam vibrations. The effectiveness of a series R–L and parallel R–L resonant shunt circuit was demonstrated theoretically and experimentally. It is observed that effective attenuations of vibration amplitudes have been achieved with decreasing the shunting resistor values for the series R–L shunt circuit and increasing the shunting resistor values in parallel R–L shunt circuit. The predictions of theoretical models have been validated experimentally. The results showed a good agreement between theory and experiment. The theoretical and experimental techniques presented in this study provide a valuable tool in the design of effective passive electrical damping.

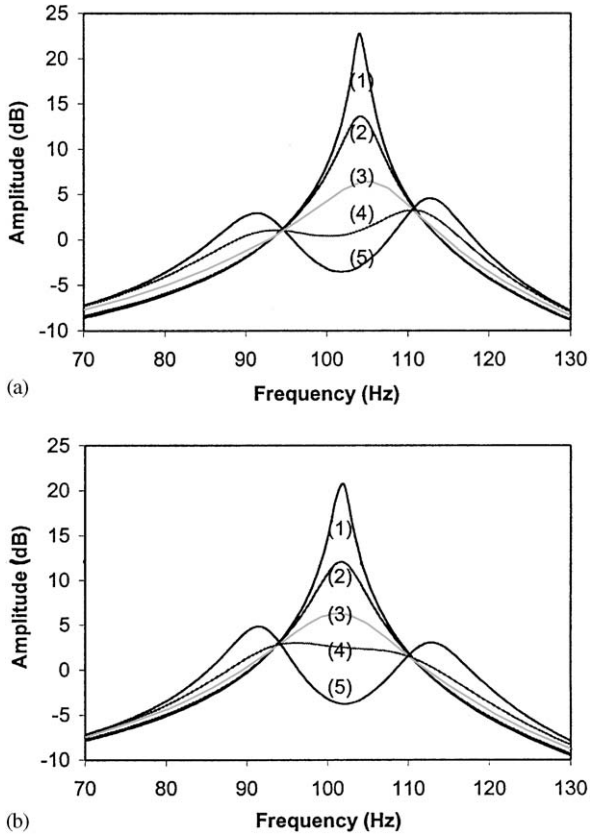

Fig. 7. Analytical transfer response function by using Eq. (37): (a) a series R–L and (b) a parallel R–L shunt circuit.

Acknowledgements

The author gratefully appreciates the financial support for this research from the Brain Korea 21 Program.

References

[1] C.H. Park, D.J. Inman, A comparison of passive electronic and mechanical damping treatments, 9th International Conference on Adaptive Structures and Technologies, Boston, MA, 1998, pp. 94–104.
[2] G. Lesieutre, Vibration damping and control using shunted piezoelectric materials, Shock and Viberation Digest 30 (1998) 187–195.
[3] N. Hagood, A. von Flotow, Damping of structural vibrations with piezoelectric materials and passive electrical networks, Journal of Sound and Vibration 146 (1991) 243–268.
[4] H. Law, P. Rossiter, G. Simon, L. Koss, Characterization of mechanical vibration damping by piezoelectric materials, Journal of Sound and Vibration 197 (1996) 489–513.
[5] M.S. Tsai, K.W. Wang, On the structural damping characteristics of active piezoelectric actuators with passive shunt, Journal of Sound and Vibration 221 (1999) 1–22.

[6] D.A. Saravanos, Damped vibration of composite plates with passive piezoelectric-resistor elements, Journal of Sound and Vibration 221 (1999) 867–885.
[7] S.J. Kim, S.H. Moon, S.K. Lee, Comparison of active and passive suppressions of nonlinear panel flutter using finite element method, 41st AIAA/ASME/ASCE/AHS/ASC Structures, Structural Dynamics, and Materials Conference, Atlanta, GA, 2000, pp. 1–9.
[8] N. Hagood, W. Chung, A. von Flotow, Modeling of piezoelectric actuator dynamics for active structural control, Journal of Intelligent Material Systems and Structures 1 (1990) 327–354.
[9] C.H. Park, D.J. Inman, Uniform model for series R–L and parallel R–L shunt circuits and power consumption, Proc. SPIE 3668: Smart Structures and Integrated Systems, Newport Beach, CA, March 1999, pp. 797–804.
[10] IEEE Std 176-1987, IEEE Standard on Piezoelectricity, The Institute of Electrical and Electronics Engineers, New York, 1987.
[11] D.J. Inman, Engineering Vibration, Prentice-Hall, Englewood Cliffs, NJ, 1996.
[12] P. Horowitz, W. Hill, The Art of Electronics, Cambridge University Press, Cambridge, 1989.